Supporting information to

"**New insight into the local structure of hydrous ferric arsenate using full-potential multiple scattering analysis, density functional theory calculations, and vibrational spectroscopy**"

Shaofeng Wang[1], Xu Ma[1], Guoqing Zhang[1], Yongfeng Jia[1,2,] *, Keisuke Hatada[3]

1. Key Laboratory of Pollution Ecology and Environmental Engineering, Institute of Applied Ecology, Chinese Academy of Sciences, Shenyang, 110016, China

2. Institute of Environmental Protection, Shenyang University of Chemical Technology, Shenyang, 100049, China

3. Département Matériaux Nanosciences, Institut de Physique de Rennes, UMR UR1-CNRS 6251, Université de Rennes 1, 35042 Rennes Cedex, France

* Corresponding author, Prof. Yonfeng Jia, Email: yongfeng.jia@iae.ac.cn, Tel: +86 24 83970503

This supporting information contains 9 figures, 4 tables, and references.

Contents

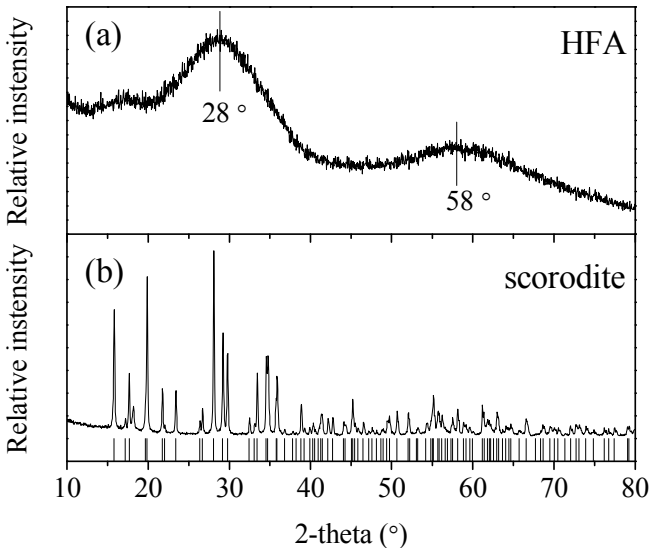

Figure S1. XRD patterns of hydrous ferric arsenate (HFA)[1, 2] (a) and scorodite (b). Vertical lines in Figure S1b is the standard of scorodite (No. 37-0468).

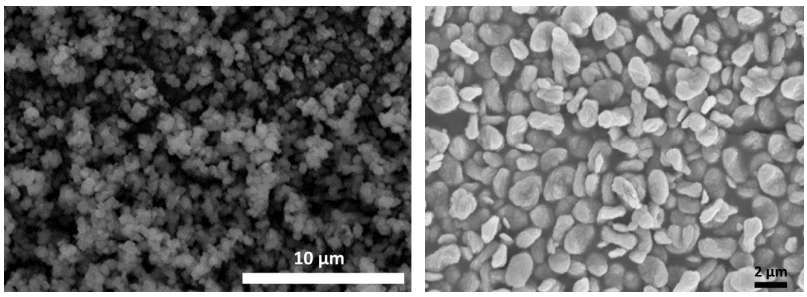

Figure S2. SEM images of synthetic HFA (left) and scorodite (right)

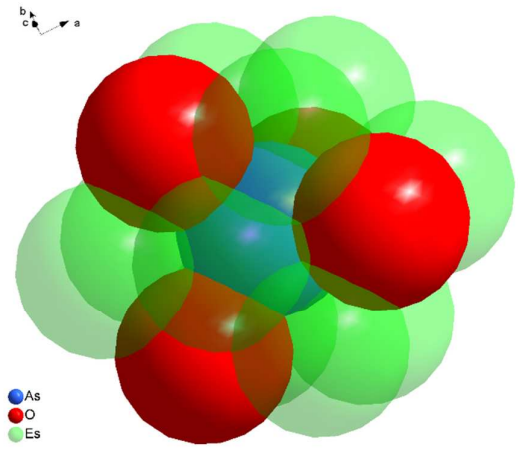

Figure S3. Wigner-Seitz cell of arsenate tetrahedron with 10 empty spheres

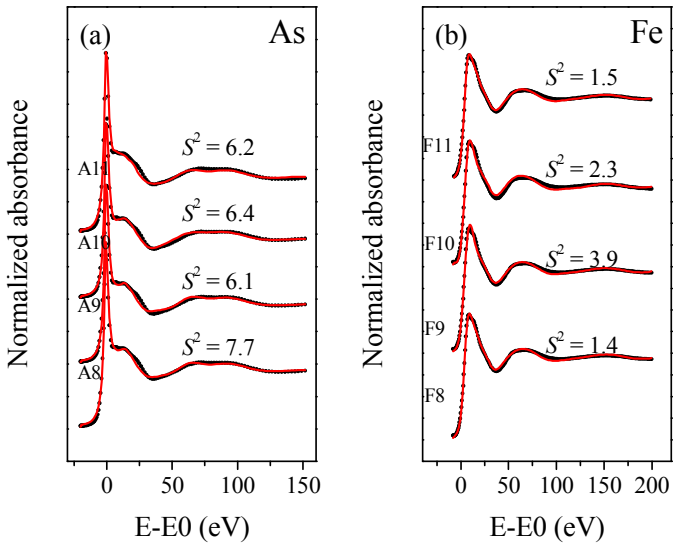

Figure S4. Comparison between non-structural optimized theoretical As (a) and Fe (b) K-edge XANES spectra (red solid lines) according to the extracted structure from scorodite (Figure 2a, b) and experimental data (black dotted lines) of HFA. For As K-edge spectra, cluster A8-A11 represent As+Fe1+Fe2+Fe3, As+Fe1+Fe2+Fe4, As+Fe1+Fe3+Fe4, and As+Fe2+Fe3+Fe4, respectively. For Fe K-edge spectra, cluster F8-F11 represent Fe+As1+As2+As3, Fe+As1+As2+As4, Fe+As1+As3+As4, and Fe+As2+As3+As4, respectively.

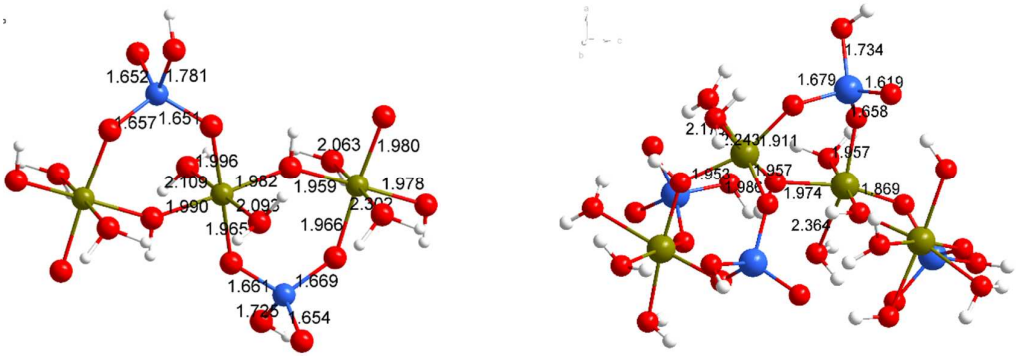

Figure S5. The butlerite-like (left) and fibroferrite-like (right) chain structures optimized by DFT calculations with S atoms replaced by As atoms. The unit of bond length marked in the figure is Å. The interatomic distances of Fe-Fe in optimized butlerite-like (left) and fibroferrite-like (right) chain structures are ~ 3.61 and ~ 3.60 Å, respectively.

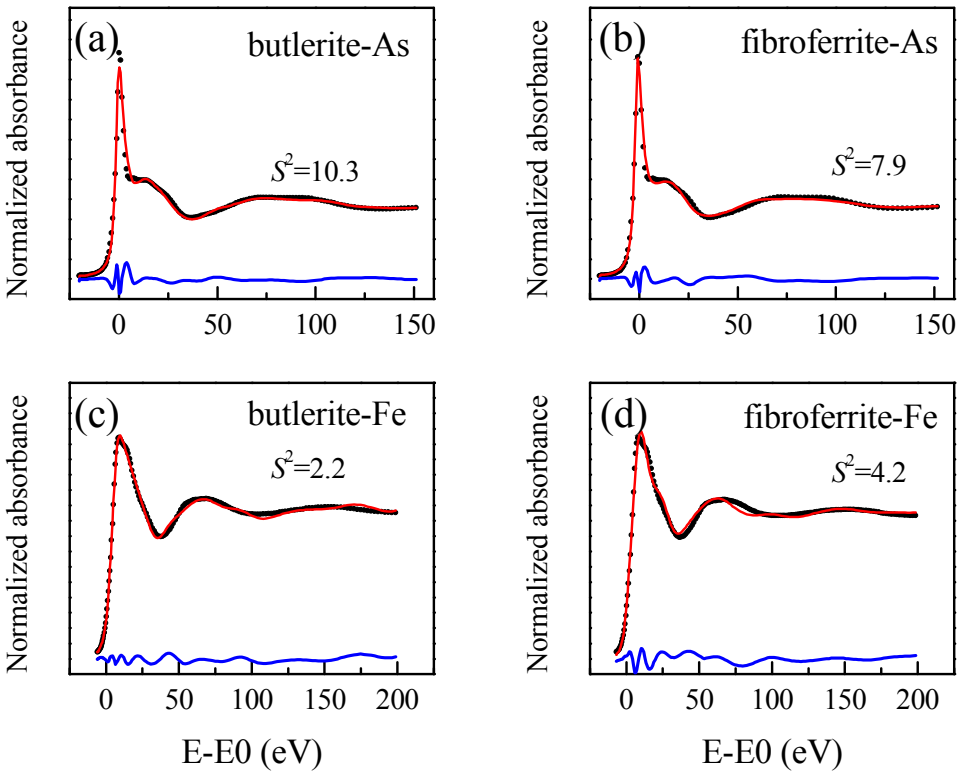

Figure S6. Comparison between theoretical and experimental data of As (a, b) and Fe (c, d) K-edge XANES spectra based on the optimized butlerite-like and fibroferrite-like HFA structures proposed by Paktunc et al.[2]

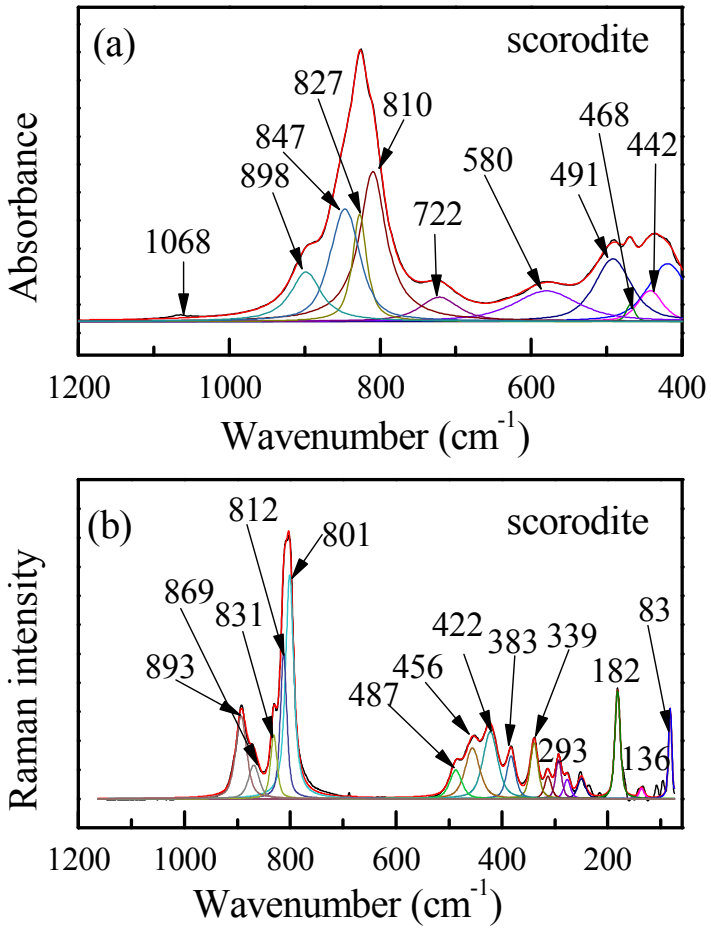

Figure S7. Deconvoluted infrared (400 – 1200 cm^{-1}) (a) and Raman (60 – 1200 cm^{-1}) (b) spectra of synthetic scorodite. Black and red line represent the experimental and fitted spectra, respectively.

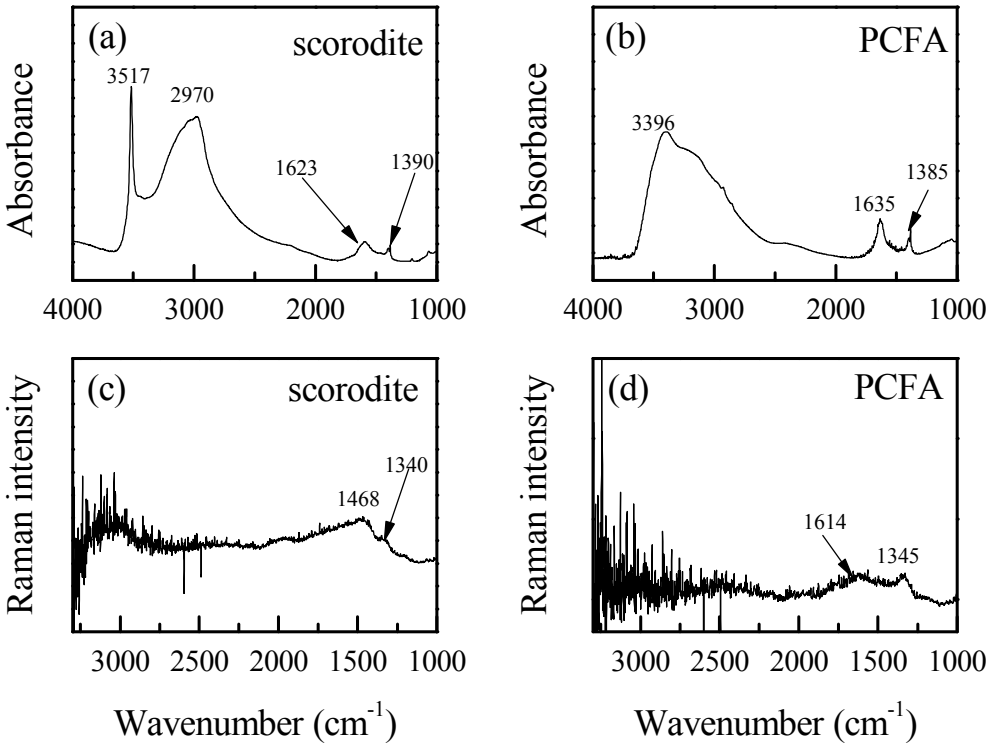

Figure S8. FTIR (top) and Raman (bottom) spectra of synthetic scorodite and HFA.

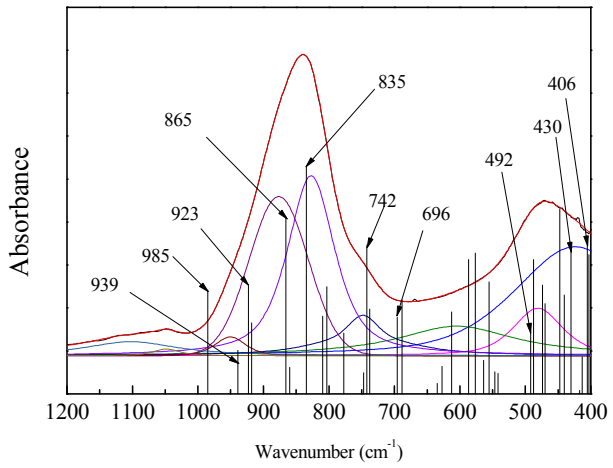

Figure S9. Comparison between experimental IR spectra and theoretical frequencies (vertical lines) of HFA in the range of 400 – 1200 cm^{-1}.

Table S1. Summary of reported values of As-Fe coordination number (CN) and averaged interatomic distance in HFA

Absorber	k range ($Å^{-1}$)	CN	Distance (Å)	Beamline	Model	Reference
As K-edge EXAFS	2.7-14	3.2	3.33	APS	scorodite	[3]
	2.7-17.55	1.85	3.31	APS	not state	[4]
	2.7-16.68	1.78	3.32	CLS	not state	[4]
	5.5-16.6	2.7	3.32	APS	not state	[4]
	5.4-15.7	2.6	3.32	CLS	not state	[4]
	3-13	1.8	3.31	APS	not state	[2]
	3-17	4[a]	3.33	ELETTRA	scorodite	[5]
	3-17	2[a]	3.33	ELETTRA	scorodite	[5]
Fe K-edge EXAFS	2.7-14	3.8	3.31	APS	not state	[3]
	2-14	4[a]	3.34	ELETTRA	scorodite	[5]
	2-14	2[a]	3.32	ELETTRA	scorodite	[5]
Total X-ray scattering	no data	no data	3.32	APS	no data	[6]

[a] The coordination number was fixed.

Table S2. Interatomic distance and bond angle in the local structure shown in Figure 2 extracted from the crystalline scorodite determined by Hawthorne.[7]

Bond	Bond length (Å) or angle (°)
As-O1	1.671 Å
As-O2	1.686 Å
As-O3	1.681 Å
As-O4	1.681 Å
As-Fe1	3.335 Å
As-Fe2	3.325 Å
As-Fe3	3.379 Å
As-Fe4	3.347 Å
Fe-O1	1.966 Å
Fe-O2	1.944 Å
Fe-O3	1.960 Å
Fe-O4	1.993 Å
Fe-OW1	2.111 Å
Fe-OW2	2.036 Å
As-O1-Fe	132.818°
As-O2-Fe	132.511°
As-O3-Fe	136.110°
As-O4-Fe	131.089°

Table S3. Fit parameters for the EXAFS data of synthetic scorodite and HFA

Sample	Path	CN[a]	R (Å)[b]	σ^2 (Å^2)[c]	ΔE (eV)[d]	S_0^2 [e]	N_{idp}/N_{var} [f]	R range (Å)	R-factor [g]	Reduced χ^2 [h]
Arsenic K-edge EXAFS										
Scorodite	As-O	4	1.69 (0)	0.003 (0)	6.6 (7)	1.0	16/9	0.9-3.3	0.009	100
	As-Fe	4	3.36 (1)	0.005 (1)						
	As-O-O	12	3.09 (5)	0.003 (6)						
	As-O-As-O	4	3.38[i]	0.004[i]						
	As-O-Fe	8	3.46 (3)	0.003 (3)						
HFA	As-O	4	1.68 (0)	0.003 (0)	7.7 (9)	1.0	16/9	0.9-3.3	0.008	110
	As-Fe	1.5	3.30 (3)	0.009 (3)						
	As-O-O	12	3.13 (4)	0.003 (3)						
	As-O-As-O	4	3.38[i]	0.004[i]						
	As-O-Fe	3	3.47 (2)	0.002 (4)						
Iron K-edge EXAFS										
Scorodite	Fe-O1	6	2.01 (0)	0.003 (0)	-4.3 (7)	0.9	20/10	1.0-3.7	0.008	34
	Fe-As	4	3.36 (1)	0.005 (1)						
	Fe-O-O	24	3.51 (6)	0.006[i]						
	Fe-O-As	8	3.48 (2)	0.003 (1)						
	Fe-O2	9	3.71 (2)	0.002 (2)						
	Fe-O-Fe-O	8	4.00[i]	0.007[i]						
HFA	Fe-O1	6	2.00 (2)	0.006 (1)	-1.4 (8)	0.9	20/10	1.0-3.7	0.006	28
	Fe-As	1.5	3.33 (1)	0.006 (1)						
	Fe-O2	4	4.09 (5)	0.007 (7)						
	Fe-O-As	3	3.50 (2)	0.003 (2)						
	Fe-O-O	24	3.45 (7)	0.010 [i]						

	Fe-O-Fe-O	6	4.11 [i]	0.011 [i]		

[a] coordination number (degeneracy), fixed. [b] mean half-path length (interatomic distance). [c] Debye-Waller parameter. [d] energy-shift. [e] amplitude reduction factor. [f] number of independent points/number of fit variables, [g] R-factor = Σ_i $(data_i\text{-}fit_i)^2/\Sigma_i$ $data_i^2$. [h] reduced χ^2 = $(N_{idp}/N_{pts}\Sigma_i$ $(data_i\text{-}fit_i)^2/\varepsilon_i)^2)/(N_{idp} - N_{var})$, where N_{pts} is the number of data points and ε_i is the uncertainty at each data point *i*. [i] Linked to the first shell. [j] defined as $(\Delta R_{As\text{-}O}+\Delta R_{As\text{-}Fe})/2$. Fit uncertainties are given for the last significant figure.

Table S4. Comparison of infrared and Raman frequencies of synthetic scorodite and HFA with theoretical frequencies of HFA and other previously reported hydrogen arsenate bearing minerals

Minerals	Infrared	Raman	Assignment
HFA [a]		213, 271	lattice mode
	424	360, 412	v_2 $HAsO_4^{2-}/H_2AsO_4^-$ symmetric bending
	481	469	v_4 $HAsO_4^{2-}/H_2AsO_4^-$ antisymmetric bending
	605		FeOH stretching vibrations/As-OH stretching vibrations from $H_2AsO_4^-$ groups
	748	766	composite of As-OH stretching vibrations from $H_2AsO_4^-$ groups and As-OFe stretching vibrations from $HAsO_4^{2-}$ groups
	827	825	composite of v_1 AsO_3 symmetric stretching vibration from $HAsO_4^{2-}$ groups and As-OFe stretching vibrations from $H_2AsO_4^-$ groups
	877	889	v_3 AsO_3 antisymmetric stretching vibration from $HAsO_4^{2-}$ groups
	951		possibly v_3 AsO_2 antisymmetric stretching vibration from $H_2AsO_4^-$ groups
	1048, 1108	985	possibly v_1 SO_4 symmetric stretching vibrations
	1385	1345	As-OH bending vibration from $HAsO_4^{2-}/H_2AsO_4^-$ groups
	1635	1614	δ H_2O bending vibrations
	3396(broad band)		composite of H_2O/OH unit/H-bond symmetric and antisymmetric stretching vibration
HFA (Theoretical) [a]	343, 406		v_2 $HAsO_4^{2-}/H_2AsO_4^-$ symmetric bending
	492		v_4 $HAsO_4^{2-}/H_2AsO_4^-$ antisymmetric bending
	577		FeOH stretching vibrations/librational modes of water molecules and hydroxyl ions
	613		As-OH stretching vibrations from $H_2AsO_4^-$ groups
	696		As-OH stretching vibrations from $HAsO_4^{2-}$ groups
	742		composite of As-OH stretching vibrations from $H_2AsO_4^-$ groups and As-OFe stretching vibrations from $HAsO_4^{2-}$ groups
	835		composite of v_1 AsO_3 symmetric stretching vibration from $HAsO_4^{2-}$ groups and As-OFe stretching vibrations from $H_2AsO_4^-$ groups
	865		v_3 AsO_3 antisymmetric stretching vibration from $HAsO_4^{2-}$ groups
	923, 939		v_3 AsO_2 antisymmetric stretching vibration from $H_2AsO_4^-$ groups

	985, 1230, 1271		As-OH bending vibration from $HAsO_4^{2-}$/$H_2AsO_4^-$ groups
	1530 – 1621		δ H_2O bending vibrations
	2804 – 3714		H_2O/OH unit/H-bond symmetric and antisymmetric stretching vibration
Scorodite $FeAsO_4$ $4H_2O$ [a, b]		83, 136, 182, 293	lattice mode
		339, 383	v_2 AsO_4^{3-} symmetric bending
	442, 468, 491	422, 456, 487	v_4 AsO_4^{3-} antisymmetric bending
	580	626	Fe-H_2O stretching vibration/librational modes of water molecules and hydroxyl ions
	722		As-O-Fe/As-OH stretching vibration
	810	801, 812	v_1 AsO_4^{3-} symmetric stretching vibration
	827, 847, 898	831, 869, 893	v_3 AsO_4^{3-} antisymmetric stretching vibration
	1068		possibly v_1 SO_4^{2-} symmetric stretching vibration
	1390, 1623	1468	δ H_2O bending vibrations
	2970, 3517		hydroxyl stretching vibrations from water molecule
Haidingerite $Ca(AsO_3OH)\cdot H_2O$ [c]		338, 323, 299	v_2 $(AsO_3OH)^{2-}$ bending vibrations
		433,420,376,369	split triply degenerate v_4 $(AsO_3OH)^{2-}$ bending vibrations
		660	librational modes of water molecules and hydroxyl ions
		739	δ AsOH bending vibration
		855	v_1 $(AsO_3OH)^{2-}$ symmetric stretching vibration
		886, 838 (shoulder), 823 (shoulder), 745	split v_3 $(AsO_3OH)^{2-}$ antisymmetric triply degenerate stretching vibration
		2842	OH stretching vibrations of water molecules
		3412, 3574	stretching vibrations of the OH units
Brassite [c]		298, 274	v_2 $(AsO_3OH)^{2-}$ bending vibrations
		448,404, 387, 358	split triply degenerate v_4 $(AsO_3OH)^{2-}$ bending vibrations
		699, 609	librational modes of water molecules and hydroxyl ions
		739	δ AsOH bending vibration
		809	v_1 $(AsO_3OH)^{2-}$ symmetric stretching vibration
		878, 876, 862	split triply degenerate v_3 $(AsO_3OH)^{2-}$ antisymmetric stretching vibration
		3035	OH stretching vibrations of water molecules
		3305, 3314, 3387,	stretching vibrations of the OH units

		3450, 3511	
Pharmacolite $Ca(AsO_3OH)\cdot 2H_2O$ [d]		125, 156	lattice vibrations
		179, 192, 209	OCaO bending modes
		287, 306	CaO stretching vibrations
		337,398	v_2 $(AsO_3OH)^{2-}$ bending mode
		416, 448	v_4 $(AsO_3OH)^{2-}$ bending mode
	668, 674	684, 542	water librational modes
	711, (737) [8]	707, (726)[8]	As-OH stretching vibrations
	826, 801		split doubly degenerate v_3 $(AsO_3OH)^{2-}$ antisymmetric stretching modes
	864, (871)[8]	865, (871)	v_1 $(AsO_3OH)^{2-}$ symmetric stretching mode
	903, 893, 841, (899)[8]	852, 886, (899)[8]	v_3 $(AsO_3OH)^{2-}$ antisymmetric stretching mode
	1120, 1163, 1190	1179	As-OH in-plane bending vibration
	1639, 1651, 1730		HOH bending modes
Arseniosiderite $Ca_2Fe_3(AsO_4)_3O_2\ H_2O$ [e]		331, 250,227,197	lattice mode
		389	v_2 $(AsO_4^{3-})/\delta_{as}(HAsO_4^{2-})$ bending mode
		479, 441	v_4 (AsO_4^{3-}) bending mode
	643	535	$FeOH_2$ stretching vibrations
		772	As-OH stretching vibrations
	778	828	v_3 (AsO_4^{3-}) antisymmetric stretching mode
		852	v_1 (AsO_4^{3-}) symmetric stretching mode
	919	927	v_1 $(HAsO_4^{2-})$ symmetric stretching mode
	1417, 1389		v_3 (CO_3^{2-}) antisymmetric stretching mode
	1624		δ H_2O bending vibration
	2851		
	3411, 3100		OH stretching / v H_2O stretching vibrations
	3576		OH stretching vibrations
burgessite, $Co_2(H_2O)_4(AsO_3OH)_2\cdot H_2O$ [f]		162	lattice mode
		233, 215	v (O–H· · ·O) stretching vibrations
		383, 353, 322	split doubly degenerate v_2 (AsO_4^{3-}) bending vibrations.
	492, 470, 437, 431	447	split triply degenerate v_4 (δ antisymmetric) (AsO_4^{3-}) bending vibrations
	589, 557		δ As-OH bending vibrations
	726, 697, 679, 655, 619		librational modes of water molecules and hydroxyl ions
	741	740	v As-OH stretching vibrations

	868, 836, 802	852, 830, 806	v_3 and v_1 (AsO_4^{3-}) stretching vibrations
	1707,1636		δ H_2O bending vibrations
	3593, 3516, 3410, 3245, 2952	3591, 3395, 3328, 3204, 3185	v OH stretching vibrations
geminite $Cu(AsO_3OH)\cdot H_2O$[g]		134, 160, 171, 178, 187	hydrogen bonding of the water molecule
		213, 244, 284, 310	Cu–O stretching and bending bands
		309, 333, 345, 364	v_2 (δ_s) $(AsO_3OH)^{2-}$ split doubly degenerate bending vibrations
		408, 424, 444, 481, 496	v_4 (δ_{as}) $(AsO_3OH)^{2-}$ split triply degenerate bending vibrations
	739, 751	741	δ As–OH bending vibrations
	804, 828, 876	812, 836, 859, 885	split triply degenerate v_3 $(AsO_3OH)^{2-}$ antisymmetric stretching vibrations
	849	851	v_1 $(AsO_3OH)^{2-}$ symmetric stretching vibration
	1240, 1306, 1361, 1541	1305	δ OH bending vibrations, overtones and combination bands
	1631, 1670		v_2 (δ) HOH bending modes
	2337, 2403, 2469	2289, 2433	the strong hydrogen bonded of water molecules
	2820, 3037, 3190, 3311	2737, 2855, 3235, 3305, 3377	the v OH stretching vibrations of hydrogen bonded watermolecules in the crystal structure
	3452, 3520	3449,3521	the OH stretching vibrations of the hydrogen bonded hydroxyls in the $(AsO_3OH)^{2-}$ units
mixite $BiCu_6(AsO_4)_3(OH)_6$ $3H_2O$[h]		386.5, 395.3, 423.1	v_2 bending modes of the $(AsO_3OH)^{2-}$ (423.1 and 395.3) and the (AsO_4^{3-}) groups (386.5)
		473.7	$v4$ antisymmetric bending mode of (AsO_4^{3-}) units.
		803,833	symmetric stretching vibration of the protonated (AsO_4^{3-}) units
		854.3, 831.5, 809.8	(AsO_4^{3-}) stretching bands
		867-870	symmetric stretching vibration of the protonated $(H_2AsO_4)^-$ units
		880-910	symmetric stretching vibration of the protonated $(HAsO_4)^{2-}$ units
		915	antisymmetric stretching vibration of protonated (AsO_4^{3-}) units
		3386.7	the interlamellar water
		3473.9, 3428.4	the OH- stretching vibration of the hydroxyl units
Na_2HAsO_4 $7H_2O$[i]	711(shoulder at	737	v As-OH stretching vibrations

	756)		
	835	825	v_1 $(AsO_3OH)^{2-}$ symmetric stretching vibration
Sainfeldite $Ca_5(HAsO_4)_2(AsO_4)_2$ $4H_2O$[i]	713	719	*v* As-OH stretching vibrations of As1-OH
	824	824	v_1 $(AsO_4^{3-})^{2-}$ symmetric stretching vibration of As2-OCa
	852	852,	v_3 (AsO_4^{3-}) antisymmetric stretching mode of As2-OCa/H_2O
	869	869,	v_1 $(AsO_3OH)^{2-}$ symmetric stretching vibration of As2-OCa
	895	895	v_3 (AsO_4^{3-}) antisymmetric stretching mode of As1-OCa
$(C_6H_9N_2)H_2AsO_4$[j]	2735 – 3402		$v(CH_3)$/ $v(NH_2)$/ v(OH)
	1792 – 2553		bands of combination and harmonics
	1748		δ OH bending vibrations
	1301 – 1667		v(C=C), v(N=C), $\delta(NH_2)$, $\delta(CH_3)$
	1184, 1240		δ(As–O–H)
	990, 1033		$v(AsO_2)$
	865, 938		$v(As(OH)_2)$
	581, 610		γ(As-O-H)
	515		$\rho(AsO_2)$ rocking
	470		$\omega(AsO_2)$ wagging
	427		δ(OHAsOH) bending
	396		$\tau(AsO_2)$ torsion
	374		δ(O-As-O) bending

[a] This study, [b] Gomez et al.[9], [c] Frost et al.[10], [d] Frost et al.[11], [e] Gomez et al.[12], [f] Čejka et al.[13], [g] Sejkora et al.[14], [h] Frost et al.[15], [i] Myneni et al.[8] [j] Chtioui et al.[16]

References

(1) Jia, Y. F.; Xu, L. Y.; Wang, X.; Demopoulos, G. P., Infrared spectroscopic and X-ray diffraction characterization of the nature of adsorbed arsenate on ferrihydrite. *Geochim Cosmochim Ac* **2007,** *71* (7), 1643-1654.

(2) Paktunc, D.; Dutrizac, J.; Gertsman, V., Synthesis and phase transformations involving scorodite, ferric arsenate and arsenical ferrihydrite: Implications for arsenic mobility. *Geochim Cosmochim Ac* **2008,** *72* (11), 2649-2672.

(3) Chen, N.; Jiang, D. T.; Cutler, J.; Kotzer, T.; Jia, Y. F.; Demopoulos, G. P.; Rowson, J. W., Structural characterization of poorly-crystalline scorodite, iron(III)-arsenate co-precipitates and uranium mill neutralized raffinate solids using X-ray absorption fine structure spectroscopy. *Geochim Cosmochim Ac* **2009,** *73* (11), 3260-3276.

(4) Jiang, D. T.; Chen, N.; Demopoulos, G. P.; Rowson, J. W., Response to the comment on "Structural characterization of poorly-crystalline scorodite, iron(III)-arsenate co-precipitates and uranium mill neutralized raffinate solids using X-ray absorption fine structure spectroscopy". *Geochim Cosmochim Ac* **2010,** *74* (15), 4597-4602.

(5) Mikutta, C.; Mandaliev, P. N.; Kretzschmar, R., New Clues to the Local Atomic Structure of Short-Range Ordered Ferric Arsenate from Extended X-ray Absorption Fine Structure Spectroscopy. *Environ Sci Technol* **2013,** *47* (7), 3122-3131.

(6) Mikutta, C.; Schröder, C.; Marc Michel, F., Total X-ray scattering, EXAFS, and Mössbauer spectroscopy analyses of amorphous ferric arsenate and amorphous ferric phosphate. *Geochim Cosmochim Ac* **2014,** *140*, 708-719.

(7) Hawthorne, F. C., The hydrogen positions in scorodite. *Acta Crystallographica, Section B (Structural Crystallography and Crystal Chemistry)* **1976,** *B32*, 2891-2.

(8) Myneni, S. C. B.; Traina, S. J.; Waychunas, G. A.; Logan, T. J., Experimental and theoretical vibrational spectroscopic evaluation of arsenate coordination in aqueous solutions, solids, and at mineral-water interfaces. *Geochim Cosmochim Ac* **1998,** *62* (19-20), 3285-3300.

(9) Gomez, M. A.; Assaaoudi, H.; Becze, L.; Cutler, J. N.; Demopoulos, G. P., Vibrational spectroscopy study of hydrothermally produced scorodite (FeAsO4 center dot 2H(2)O), ferric arsenate sub-hydrate (FAsH; $FeAsO_4 \cdot 0.75H_2O$) and basic ferric arsenate sulfate (BFAS; $Fe[(AsO_4)_{(1-x)}(SO_4)_{(x)}(OH)_{(x)}] \cdot wH_{(2)}O$). *J Raman Spectrosc* **2010,** *41* (2), 212-221.

(10) Frost, R. L.; Bahfenne, S.; Čejka, J.; Sejkora, J.; Palmer, S. J.; Škoda, R., Raman microscopy of haidingerite $Ca(AsO_3OH) \cdot H_2O$ and brassite $Mg(AsO_3OH) \cdot 4H_2O$. *J Raman Spectrosc* **2010,** *41* (6), 690-693.

(11) Frost, R. L.; Bahfenne, S.; Čejka, J.; Sejkora, J.; Plášil, J.; Palmer, S. J., Raman spectroscopic study of the hydrogen-arsenate mineral pharmacolite $Ca(AsO_3OH) \cdot 2H_2O$—implications for aquifer and sediment remediation. *J Raman Spectrosc* **2010,** *41* (10), 1348-1352.

(12) Gomez, M. A.; Becze, L.; Blyth, R. I. R.; Cutler, J. N.; Demopoulos, G. P., Molecular and structural investigation of yukonite (synthetic & natural) and its

relation to arseniosiderite. *Geochim Cosmochim Ac* **2010,** *74* (20), 5835-5851.

(13) Čejka, J.; Sejkora, J.; Bahfenne, S.; Palmer, S. J.; Plášil, J.; Frost, R. L., Raman spectroscopy of hydrogen-arsenate group (AsO_3OH) in solid-state compounds: cobalt mineral phase burgessite $Co_2(H_2O)_4[AsO3OH]_2 \cdot H_2O$. *J Raman Spectrosc* **2011,** *42* (2), 214-218.

(14) Sejkora, J.; Čejka, J.; Frost, R. L.; Bahfenne, S.; Plášil, J.; Keeffe, E. C., Raman spectroscopy of hydrogen-arsenate group (AsO_3OH) in solid-state compounds: copper mineral phase geminite $Cu(AsO_3OH) \cdot H_2O$ from different geological environments. *J Raman Spectrosc* **2010,** *41* (9), 1038-1043.

(15) Frost, R. L.; Weier, M.; Martins, W.; Duong, L., Identification of mixite minerals - An SEM and Raman spectroscopic analysis. *Mineral Mag* **2005,** *69* (2), 169-177.

(16) Chtioui, A.; Benhamada, L.; Jouini, A., Crystal structure, thermal analysis and IR spectroscopic investigation of $(C_6H_9N_2)H_2XO_4$ (X = As, P). *Mater Res Bull* **2005,** *40* (12), 2243-2255.